JACS
JOURNAL OF THE AMERICAN CHEMICAL SOCIETY
Article
pubs.acs.org/JACS

Aerobic Dehydrogenation of Cyclohexanone to Cyclohexenone Catalyzed by $Pd(DMSO)_2(TFA)_2$: Evidence for Ligand-Controlled Chemoselectivity

Tianning Diao, Doris Pun, and Shannon S. Stahl*

Department of Chemistry, University of Wisconsin−Madison, 1101 University Avenue, Madison, Wisconsin 53706, United States

Supporting Information

ABSTRACT: The dehydrogenation of cyclohexanones affords cyclohexenones or phenols via removal of 1 or 2 equiv of H_2, respectively. We recently reported several Pd^{II} catalyst systems that effect aerobic dehydrogenation of cyclohexanones with different product selectivities. $Pd(DMSO)_2(TFA)_2$ is unique in its high chemoselectivity for the conversion of cyclohexanones to cyclohexenones, without promoting subsequent dehydrogenation of cyclohexenones to phenols. Kinetic and mechanistic studies of these reactions reveal the key role of the dimethylsulfoxide (DMSO) ligand in controlling this chemoselectivity. DMSO has minimal kinetic influence on the rate of $Pd(TFA)_2$-catalyzed dehydrogenation of cyclohexanone to cyclohexenone, while it strongly inhibits the second dehydrogenation step, conversion of cyclohexenone to phenol. These contrasting kinetic effects of DMSO provide the basis for chemoselective formation of cyclohexenones.

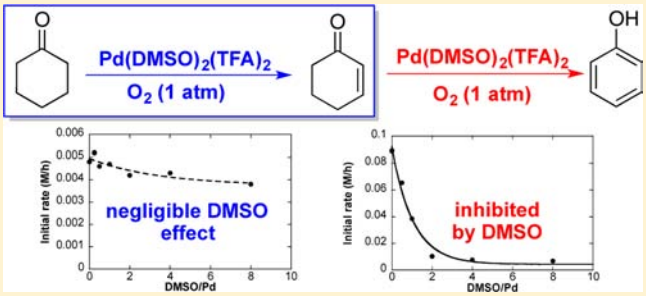

INTRODUCTION

Dehydrogenation of saturated C−C bonds represents an important class of C−H functionalization reactions. Homogeneous catalysts, such as iridium/PCP-pincer complexes, have been investigated extensively for such transformations, and they have proven to be quite effective in the conversion of alkanes to alkenes or arenes.[1,2] These reactions are performed with a sacrificial H_2 acceptor, such as *tert*-butylethylene, or under "acceptorless" conditions, in which H_2 is physically removed from the reaction mixture. Oxidative dehydrogenation, using O_2 as the hydrogen acceptor, represents an appealing alternative method to introduce sites of unsaturation into organic molecules. The majority of precedents in this area, however, feature high-temperature, gas-phase conditions for commodity chemical applications. Prominent targets include the conversion of ethane to ethylene, propane to propylene, or ethylbenzene to styrene.[3] The reaction methods and conditions for these transformations are unsuitable for use with fine chemicals, pharmaceuticals, or related molecules bearing diverse functional groups. Homogeneous Pd^{II} catalysts could find utililty in such applications; however, precedents are quite limited.[4−6] Until recently, little effort has been made to expand the scope and synthetic utility of such reactions.[7]

We recently reported three different catalyst systems that promote aerobic dehydrogenation of cyclohexanones and other carbonyl compounds (Chart 1). A $Pd(TFA)_2$/2-Me_2Npy (TFA = trifluoroacetate, 2-Me_2Npy = 2-dimethylaminopyridine) catalyst system exhibits good activity for the dehydrogenation of cyclohexanones and cyclohexenones to phenols.[8] A $Pd(TFA)_2$/4,5-diazafluorenone catalyst exhibits similar reactivity, but is especially useful for α,β-dehydrogenation of heterocyclic carbonyl compounds and exhibits some success in the dehydrogenation of acyclic carbonyl compounds.[9,10] Finally, a $Pd(DMSO)_2(TFA)_2$ (DMSO = dimethylsulfoxide) catalyst enables selective dehydrogenation of cyclohexanones to cyclohexenones.[11] The reactions mediated by these catalysts provide compelling routes to substituted phenols and/or enones, and they serve as an important foundation for the development of other aerobic dehydrogenation methods. A number of related transformations, including reactions for the synthesis of aryl ethers and anilines from cyclohexanones and cyclohexenones, have been reported by other groups over the past year.[12]

Further development of oxidative dehydrogenation reactions of this type would benefit from mechanistic insights. The catalytic dehydrogenation of a cyclohexanone could lead to cyclohexenone and/or phenol products, and, in the reaction of unsubstituted cyclohexanone, the three catalyst systems in Chart 1 exhibit different selectivity patterns (Scheme 1). The first two catalysts systems, $Pd(TFA)_2$/2-Me_2Npy and $Pd(TFA)_2$/diazafluorenone, favor formation of phenol, whereas $Pd(DMSO)_2(TFA)_2$ promotes highly selective formation of cyclohexenone. Kinetic modeling of the reaction time courses has been used to obtain relative rate constants for the first and second dehydrogenation steps with each of these catalyst systems (Scheme 1B).[13] The results show that the first two catalyst systems promote dehydrogenation of cyclohexenone to

Received: March 29, 2013
Published: May 13, 2013

   dx.doi.org/10.1021/ja4031648 | J. Am. Chem. Soc. 2013, 135, 8205−8212

Chart 1. Pd Catalysts and Representative Products of Aerobic Dehydrogenation of Carbonyl Compounds

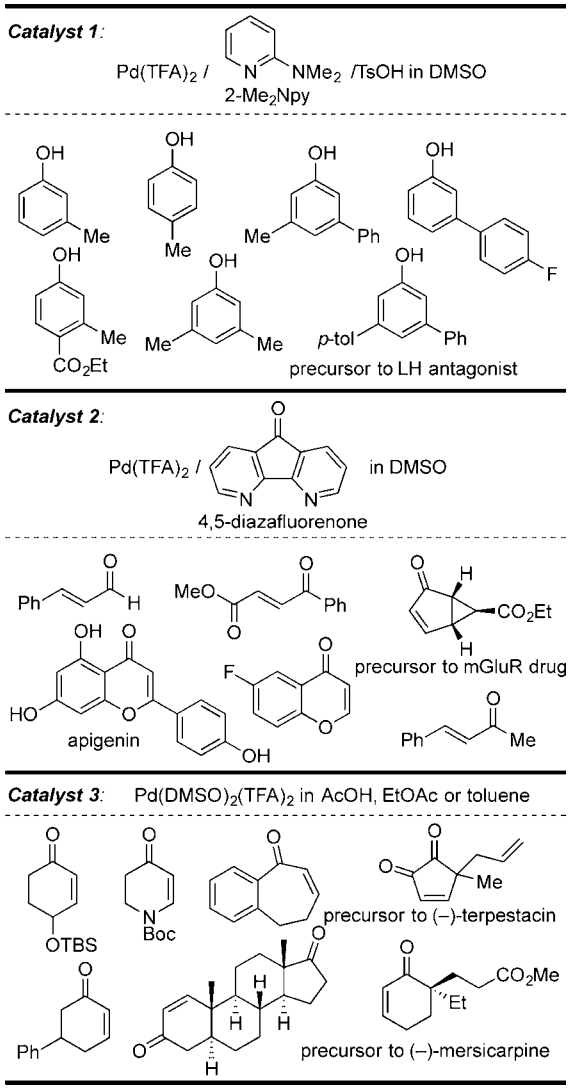

Scheme 1. Relative Rate Constants for Different Catalyst Systems in the Dehydrogenation of Cyclohexanone

(A)

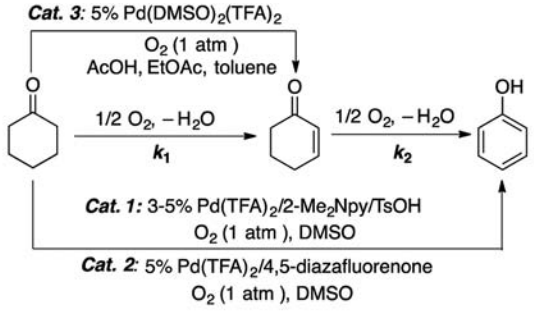

(B)

Catalyst	Solvent	k_1/k_2
Cat. 1: $Pd(TFA)_2$/**2-Me_2Npy**/TsOH	DMSO	0.61
Cat. 2: $Pd(TFA)_2$/**4,5-diazafluorenone**	DMSO	0.36
Cat. 3: $Pd(DMSO)_2(TFA)_2$	AcOH, EtOAc, toluene	>10

phenol more rapidly than cyclohexanone to cyclohexenone (i.e., $k_1/k_2 < 1$; Scheme 1B). The opposite trend is observed with $Pd(DMSO)_2(TFA)_2$ as the catalyst (k_1/k_2 = 10–33, depending on the solvent[14]). These kinetic differences have important synthetic implications, as the k_1/k_2 ratio with $Pd(DMSO)_2(TFA)_2$ is sufficiently high that excellent yields of cyclohexenone products can be obtained for a wide range of substrates, with minimal phenol byproducts.[11]

A plausible catalytic cycle for dehydrogenation of cyclohexanone derivatives involves formation of a Pd^{II}-enolate followed by β-hydride elimination (steps 1 and 2, Scheme 2).

Scheme 2. Proposed Mechanism for Pd-Catalyzed Dehydrogenation of Cyclohexanones

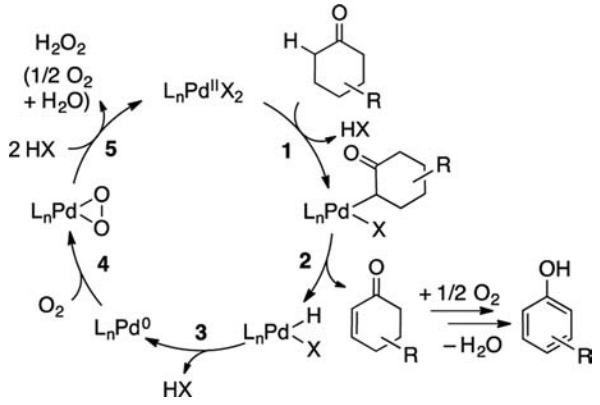

This sequence is analogous to that proposed for Saegusa-type dehydrosilylation of silyl enol ethers.[15] Oxidation of the Pd^{II}-hydride intermediate is expected to proceed via Pd^0, as has been demonstrated for well-defined model systems (steps 3–5).[16] A similar catalytic cycle can be proposed for the dehydrogenation of cyclohexenone to phenol.

The simplified analysis above does not account for the different selectivity patterns observed with the different catalyst systems in Scheme 1. Here, we present a kinetic and mechanistic investigation of $Pd(DMSO)_2(TFA)_2$-catalyzed dehydrogenation of cyclohexanone to cyclohexenone, and this work sheds light on three key mechanistic issues: (1) the identity of the turnover-limiting step; (2) the role of ligand in the catalyst system; (3) the origin of the chemoselectivity for enone relative to phenol. The results show that DMSO serves as a ligand that stabilizes a homogeneous Pd^{II} catalyst and that inhibits conversion of cyclohexenone to phenol. These results complement a companion study of $Pd(TFA)_2$/2-Me_2Npy-catalyzed dehydrogenation of cyclohexanone, in which the Pd^{II} catalyst is found to undergo in situ conversion into Pd nanoparticles that facilitate full dehydrogenation of cyclohexanone to phenol.[17]

RESULTS AND DISCUSSION

Kinetic Studies of $Pd(DMSO)_2(TFA)_2$-Catalyzed Oxidation of Cyclohexanone. The catalytic dehydrogenation of cyclohexanone with $Pd(DMSO)_2(TFA)_2$ in EtOAc (eq 1)

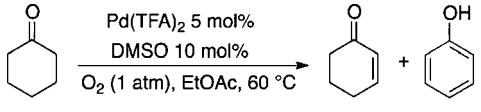

(1)

dx.doi.org/10.1021/ja4031648 | J. Am. Chem. Soc. 2013, 135, 8205–8212

proceeds smoothly and reaches complete conversion after approximately 24 h at 60 °C under 1 atm O_2 (Figure 1). The

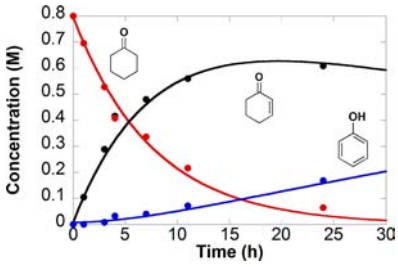

Figure 1. Reaction time course of $Pd(DMSO)_2(TFA)_2$-catalyzed aerobic dehydrogenation of cyclohexanone. Estimated standard deviation for individual points: ≤5%. Reaction conditions: [cyclohexanone] = 0.8 M (0.8 mmol), $[Pd(TFA)_2]$ = 0.04 M (0.04 mmol), [DMSO] = 0.08 M (0.08 mmol), O_2 (1 atm), EtOAc (1 mL), 60 °C.

time course data fit well to an A→B→C kinetic model (Figure 1). Good mass balance reveals that negligible side reactions occur. The rate constants for the first (k_1) and second (k_2) oxidation steps are estimated to be 0.13 and 0.013 h^{-1}, respectively, resulting in a ratio of k_1/k_2 = 10. Higher selectivity can be achieved in other solvents (e.g., k_1/k_2 = 33 in AcOH), but use of the lower-selectivity solvent EtOAc was chosen for the present studies to facilitate study of both dehydrogenation steps.

The lack of an induction period in the reaction time course for $Pd(DMSO)_2(TFA)_2$-catalyzed dehydrogenation of cyclohexanone allowed us to employ initial-rates methods to determine the kinetic orders of each reaction component. The conversion of cyclohexenone to phenol is negligible within the first two turnovers, and the concentration of cyclohexenone was monitored by gas chromatography to determine the initial rates. The reaction exhibits a first-order dependence on [cyclohexanone] and $[Pd(DMSO)_2(TFA)_2]$ (Figure 2).

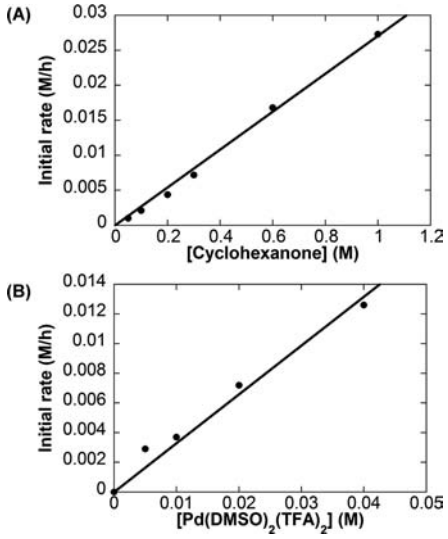

Figure 2. Kinetic orders for $Pd(DMSO)_2(TFA)_2$-catalyzed dehydrogenation of cyclohexanone to cyclohexenone: dependence of the initial rate on (A) substrate concentration and (B) $Pd(DMSO)_2(TFA)_2$ concentration. Estimated standard deviation for individual points: ≤ 5%. Reaction conditions: EtOAc (1 mL), O_2 (1 atm), 60 °C; (A) $[Pd(TFA)_2]$ = 0.01 M (0.01 mmol), [DMSO] = 0.02 M (0.02 mmol); (B) [cyclohexanone] = 0.2 M (0.2 mmol).

Systematic analysis of the O_2-pressure dependence was complicated by Pd-black formation at lower pO_2; however, increasing the O_2 pressure from 1.7 to 3.2 atm had minimal impact on the rate, consistent with a zero-order dependence on O_2 (Figure S1).

Variation of [DMSO] at fixed [cyclohexanone] and $[Pd(TFA)_2]$ reveals that increasing the quantity of DMSO has only a minor inhibitory effect on the reaction rate (Figure 3A).

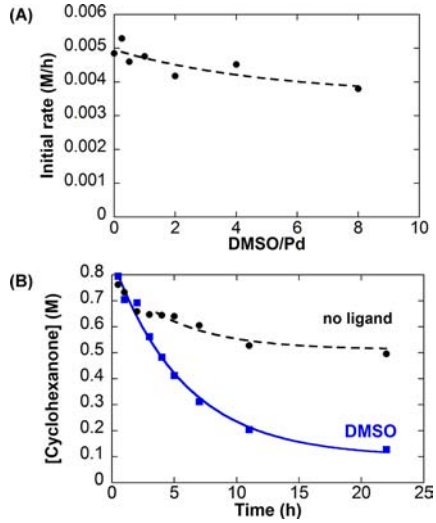

Figure 3. (A) Effect of the DMSO ligand on Pd-catalyzed dehydrogenation of cyclohexanone to cyclohexenone evident from the dependence of the initial rate on the DMSO/Pd ratio. (B) Comparison of time courses for the dehydrogenation of cyclohexanone in the absence or presence of DMSO. Estimated standard deviation for individual points: ≤ 5%. Reaction conditions: EtOAc (1 mL), O_2 (1 atm), 60 °C; (A) [cyclohexanone] = 0.2 M (0.2 mmol), $[Pd(TFA)_2]$ = 0.01 M (0.01 mmol); (B) [cyclohexanone] = 0.8 M (0.8 mmol), $[Pd(TFA)_2]$ = 0.04 M (0.04 mmol), [DMSO] (when present) = 0.08 M (0.08 mmol) (blue).

Comparison of the time courses in the absence and presence of 2 equiv of DMSO, however, reveals that the catalyst undergoes rapid deactivation in the absence of DMSO (Figure 3B). Concomitant formation of Pd-black is observed under these ligandless conditions. Minimal Pd-black formation is observed with ≥2 equiv of DMSO.

Deuterium kinetic isotope effects (KIEs) were determined by independent measurements of the initial rates with the protio, α-deuterated (cyclohexanone-d_4), and fully deuterated (cyclohexanone-d_{10}) substrates (Figure 4). Cyclohexanone reacts 2.9(±0.27) times faster than cyclohexanone-d_4, reflecting a primary KIE for cleavage of the α-C−H. The reaction time courses for cyclohexanone-d_4 and cyclohexanone-d_{10} are nearly identical, and the ratio of the rates, 1.1(±0.20), reflects a negligible KIE for cleavage of the β-hydrogen atom (Figure 4). GC-MS and ^{1}H NMR spectroscopic analyses reveal that no proton incorporation takes place into the α position under the reaction conditions. The intrinsic KIE for α-C−H cleavage was obtained from an intramolecular competition experiment with spiro[4,5]decan-6-one-7-d_1 (eq 2). The corresponding enone is formed slowly as the sole product. After 24 h, a 13% yield of enone is obtained, with the H/D products obtained in a ratio of 1:2.7, corresponding to a nearly identical KIE relative to that obtained from the independent rate measurements.

dx.doi.org/10.1021/ja4031648 | J. Am. Chem. Soc. 2013, 135, 8205−8212

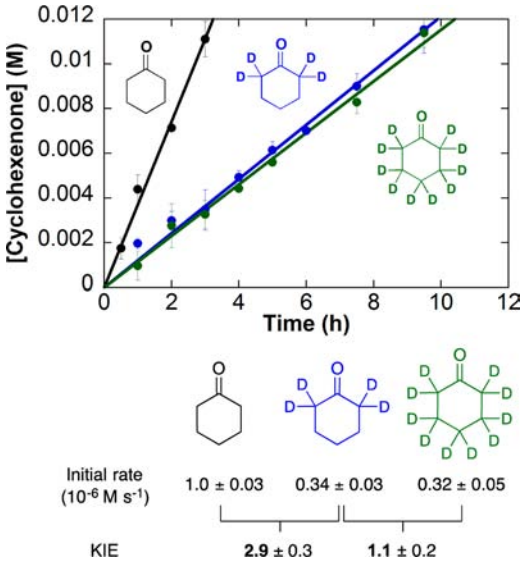

Figure 4. Deuterium kinetic isotope effects derived from independent initial rates measurements for dehydrogenation of cyclohexanone (performed in triplicate). The plots are labeled with the corresponding cyclohexanone-d_n substrate. Estimated standard deviation for individual points: ≤ 5%. Reaction conditions: [Substrate] = 0.2 M (0.2 mmol), [$Pd(TFA)_2$] = 0.01 M (0.01 mmol), [DMSO] = 0.02 M (0.02 mmol), EtOAc (1 mL), O_2 (1 atm), 60 °C.

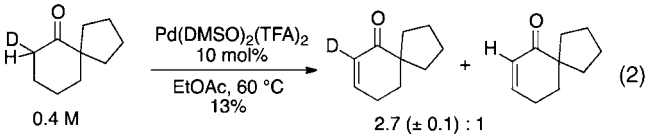

Replacement of $Pd(TFA)_2$ with $Pd(OAc)_2$ leads to reduced initial rate (Figure 5). When a mixture of $Pd(TFA)_2$ and

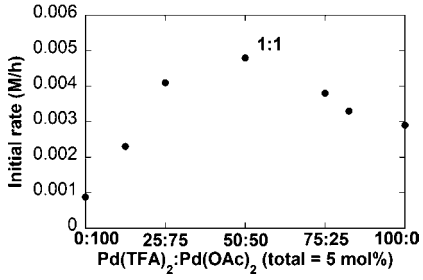

Figure 5. Dependence of the initial rate of Pd-catalyzed oxidation of cyclohexanone on different anionic ligands of Pd. Estimated standard deviation for individual points: ≤ 5%. Reaction conditions: [cyclohexanone] = 0.2 M (0.2 mmol), $[Pd]_{total}$ = 0.01 M (0.01 mmol), [DMSO] = 0.02 M (0.02 mmol), EtOAc (1 mL), O_2 (1 atm), 60 °C.

$Pd(OAc)_2$ is used as the Pd source, maintaining the total [Pd] at 5 mol %, increased initial rates are observed. The maximum rate was observed at an acetate:trifluoroacetate ratio of 1:1.

$Pd(DMSO)_2(TFA)_2$-Catalyzed Dehydrogenation of Cyclohexenone to Phenol. Cyclohexenone-to-phenol dehydrogenation proceeds very slowly under the conditions of $Pd(DMSO)_2(TFA)_2$-catalyzed dehydrogenation of cyclohexanones (cf. Scheme 1), but independent insights into cyclohexenone reactivity could be obtained by increasing the catalyst loading from 5 to 10 mol % (eq 3), and increasing the substrate concentration from 0.2 to 0.8 M. In contrast to the well-

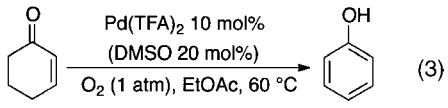

behaved kinetics observed for cyclohexanone-to-cyclohexenone dehydrogenation, the cyclohexenone-to-phenol reaction exhibits an induction period and a sigmoidal time course for formation of phenol (Figures 6 and S6). Control reactions with

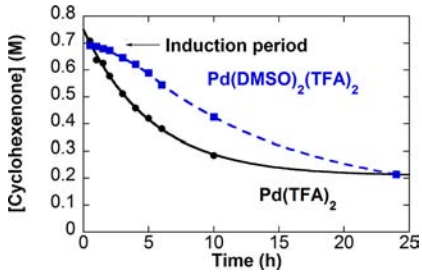

Figure 6. Time courses of $Pd(TFA)_2$-catalyzed dehydrogenation of cyclohexenone to phenol in the presence (blue) or absence (black) of DMSO. Estimated standard deviation for individual points: ≤5%. Reaction conditions: [cyclohexenone] = 0.8 M (0.8 mmol), [$Pd(TFA)_2$] = 0.08 M (0.08 mmol), [DMSO] (when present) = 0.16 M (0.16 mmol), EtOAc (1 mL), O_2 (1 atm), 60 °C.

10 mol % phenol or H_2O added to the initial reaction mixture exhibit identical rates (Figure S8), indicating that the sigmoidal time course does not arise from product-induced autocatalysis.

Pd-black is observed after the reaction, but the reaction mixture remains deep yellow, suggesting that the Pd^{II} catalyst is partially retained in solution. If $Pd(TFA)_2$ is used as the catalyst (i.e., in the absence of DMSO), cyclohexenone dehydrogenation proceeds without an induction period to high conversion. More Pd-black formation is observed relative to the reaction in the presence DMSO, and the solution is colorless after 24 h, suggesting near-complete conversion of Pd^{II} into Pd-black during the reaction. The Pd-black obtained from the reaction mixture is not an effective catalyst for the reaction.[18] More thorough analysis of the effect of DMSO on the reaction reveals that increasing the [DMSO] has a significant inhibitory effect on the rate of phenol formation (Figure 7). Similarly, higher [DMSO] increases the length of the induction period (Figures 8 and S6 and Table S1). Collectively, these results are consistent with formation of Pd nanoparticles or intermediate-sized aggregates under the reaction conditions that exhibit

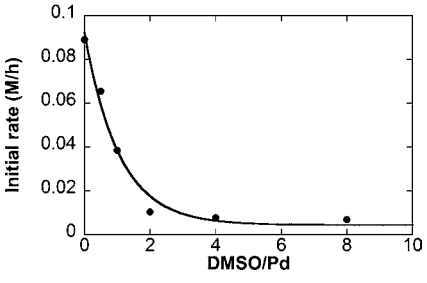

Figure 7. Dependence of the initial rate (i.e., during the induction period) of Pd-catalyzed dehydrogenation of cyclohexenone to phenol on the DMSO/Pd ratio. Estimated standard deviation for individual points: ≤ 5%. Reaction conditions: [cyclohexenone] = 0.8 M (0.8 mmol), [$Pd(TFA)_2$] = 0.08 M (0.08 mmol), EtOAc (1 mL), O_2 (1 atm), 60 °C.

dx.doi.org/10.1021/ja4031648 | J. Am. Chem. Soc. 2013, 135, 8205−8212

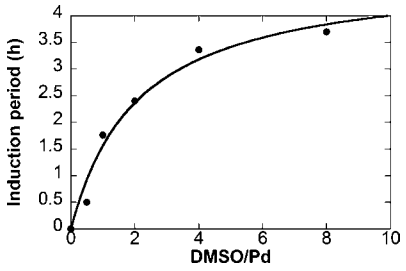

Figure 8. Dependence of the length of induction period on the Pd-catalyzed dehydrogenation of cyclohexenone to phenol on [DMSO]. Estimated standard deviation for individual points: ≤10%. Reaction conditions: [cyclohexenone] = 0.8 M (0.8 mmol), $[Pd(TFA)_2]$ = 0.08 M (0.08 mmol), EtOAc (1 mL), O_2 (1 atm), 60 °C.

higher activity than Pd^{II} for the dehydrogenation of cyclohexenone (see further discussion below). The inhibitory effect of DMSO can be attributed to its ability to stabilize the homogeneous Pd^{II} catalyst and slow formation of these particles.

Cyclohexenone dehydrogenation by Pd^{II} could be initiated by activation of the C−H bond at the 4- or 6-position of the ring, as relevant precedents exist for both. For example, deprotonation of cyclohexenone by lithium diisopropylamide (LDA) affords 2-oxylcyclohexa-1,3-dienyllithium (eq 4),[19,20]

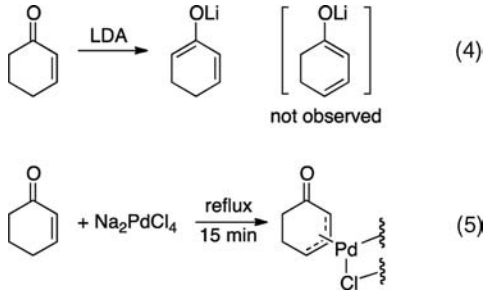

and deuterated Brønsted acids lead to isotopic scrambing of the α-C−H position, leaving the allylic C−H position unaffected.[21] In contrast, cyclohexenone reacts with sodium tetrachloropalladate to afford a dimeric π-allyl-Pd^{II} species, corresponding to cleavage of the allylic C−H bond (eq 5).[22,23] Imahori et al. recently reported a Pd-catalyzed C−H arylation−aromatization of cyclohexenone that furnishes 4-arylphenol derivatives, again consistent with Pd-mediated cleavage of the allylic C−H bond.[12b]

Isotopically labeled cyclohexenones were prepared to probe the site of C−H cleavage in $Pd(DMSO)_2(TFA)_2$-catalyzed dehydrogenation of cyclohexenone.[24] Initial rates were monitored for reactions of cyclohexenone-d_0, 2,6,6-cyclohexenone-d_3, and 2,4,4,6,6-cyclohexenone-d_5 under the standard reaction conditions (Figure 9). The unlabeled cyclohexanone exhibits a rate 2.9-fold faster than the two deuterium-labeled substrates, both of which react with identical rates. These data indicate the presence of a primary KIE (2.9 ± 0.2) associated with cleavage of the α-C−H bond in the conversion of cyclohexenone to phenol, which not only establishes the site of C−H cleavage, but also reveals that this step is rate-determining in Pd-mediated dehydrogenation of cyclohexenone.

Mechanistic Analysis. *A. DMSO Ligand-Controlled Chemoselectivity in the Dehydrogenation of Cyclohexanone.* The mechanistic data presented above provide a number

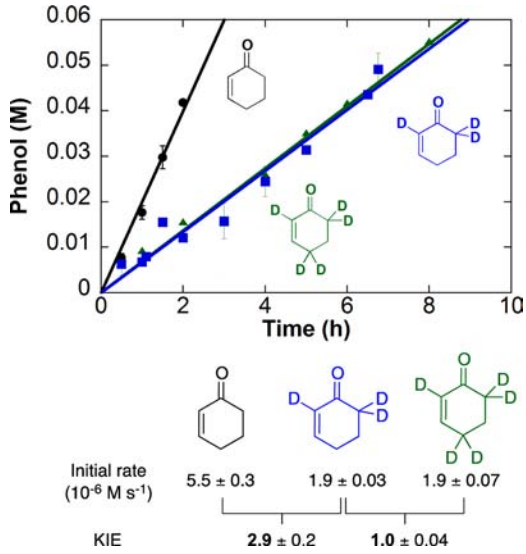

Figure 9. Deuterium kinetic isotope effects for dehydrogenation of cyclohexenone to phenol derived from independent measurement of initial rates (performed in triplicate). The plots are labeled with the corresponding cyclohexenone-d_n substrate. Reaction conditions: [substrate] = 0.8 M (0.4 mmol), $[Pd(TFA)_2]$ = 0.04 M (0.02 mmol), [DMSO] = 0.08 M (0.04 mmol), EtOAc (1 mL), O_2 (1 atm), 60 °C.

of insights into the $Pd(DMSO)_2(TFA)_2$-catalyzed dehydrogenation of cyclohexanone. Perhaps most striking is the dramatically different effects of DMSO on the cyclohexanone-to-cyclohexenone and cyclohexenone-to-phenol dehydrogenation steps. DMSO has negligible impact on the rate of the first reaction (Figure 3A), but it strongly inhibits the second (Figure 7). These contrasting effects provide the basis for selective formation of cyclohexenone, rather than phenol, in the catalytic reaction.

The inhibitory effect of DMSO on cyclohexenone-to-phenol dehydrogenation is attributed to two factors: (1) a dramatic decrease in the initial rate (Figure 7) and (2) an increase in the length of the induction period (Figure 8) with increasing [DMSO]. The effect of [DMSO] on the initial rate can be explained by DMSO dissociation from Pd^{II} prior to activation of cyclohexenone, while the effect of [DMSO] on the induction period appears to be associated with Pd aggregation into Pd nanoparticles and Pd-black. DMSO serves as a stabilizing ligand for the homogeneous catalyst, inhibiting Pd aggregation. This effect is needed to achieve high conversion in the dehydrogenation of cyclohexanone to cyclohexenone (cf. Figure 3B). In contrast, dehydrogenation of cyclohexenone to phenol appears to benefit from catalyst aggregation, as reflected by the enhanced rate following the induction period. The latter reaction proceeds most rapidly under ligand-free conditions, in the absence of DMSO.

The sigmoidal time course observed for cyclohexenone-to-phenol dehydrogenation in the presence of DMSO (Figure 6) resembles reactions that undergo in situ transformation of a molecular catalyst-precursor into catalytically active nanoparticles.[25] Pd nanoparticle formation has been characterized recently in the $Pd(TFA)_2$/2-Me_2Npy-catalyzed dehydrogenation of cyclohexanone to phenol,[17] and the Pd nanoparticles were found to be more active than the Pd^{II} catalyst precursor for dehydrogenation of cyclohexenone. Extrapolation of these results to the present catalyst system supports the proposal that

dx.doi.org/10.1021/ja4031648 | J. Am. Chem. Soc. 2013, 135, 8205−8212

the inhibitory effect of DMSO on the cyclohexenone-to-phenol step (cf. Figure 7) arises from DMSO stabilization of homogeneous Pd and inhibition of Pd nanoparticle formation. Thus, the high selectivity for enone formation with Pd(DMSO)$_2$(TFA)$_2$ appears to correlate with the presence of a (relatively) stable homogeneous Pd^{II} catalyst.

B. Mechanism of Pd(DMSO)$_2$(TFA)$_2$-Catalyzed Dehydrogenation of Cyclohexanone. We recently characterized the solution-phase structure of Pd(DMSO)$_2$(TFA)$_2$ in a number of different solvents.[26] In EtOAc, this complex exists as an equilibrium mixture of *S,S*- and *S,O*-ligated bis-DMSO complexes (eq 6). Pd(DMSO)$_2$(TFA)$_2$-catalyzed dehydrogenation of cyclohexanone is envisioned to proceed by a series of three steps (Scheme 3): (i) formation of a Pd^{II}-cyclohexanone adduct, (ii) cleavage of the α-C−H bond, with concomitant loss of TFAH, to afford a Pd^{II}-enolate species, and (iii) β-hydride elimination to afford the cyclohexenone product and a Pd^{II}-hydride.

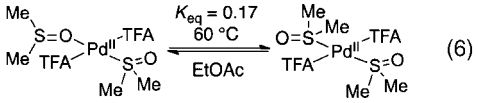

(6)

Scheme 3. Proposed Mechanism for Pd(DMSO)$_2$(TFA)$_2$-Catalyzed Dehydrogenation of Cyclohexanone

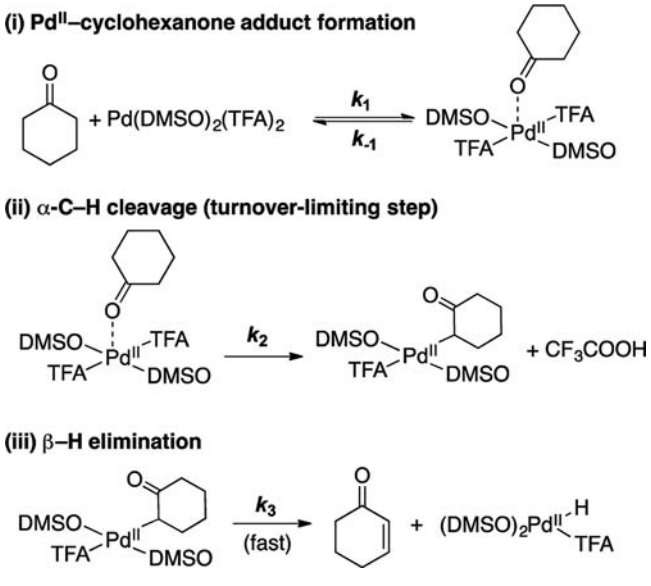

An alternative pathway for the formation of the Pd^{II}-enolate species could involve reversible ketone-enol tautomerization, followed by activation of the enol by Pd^{II} (eq 7). This mechanism would resemble that of Saegusa-type oxidations of silyl enol ethers;[15] however, it is not consistent with the significant primary KIE observed here (cf. Figure 4).

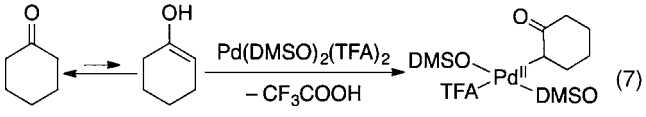

(7)

The experimental data reveal a first-order kinetic dependence on [cyclohexanone] and [Pd(DMSO)$_2$(TFA)$_2$]. Whereas a primary KIE is observed for cleavage of the α-C−H bond, no KIE is observed for cleavage of the β-hydrogen atom. These data are consistent with steady-state formation of the Pd^{II}-cyclohexanone adduct followed by turnover-limiting cleavage of the α-C−H bond, as proposed in Scheme 3, steps i and ii.

The minimal effect of DMSO on the reaction rate suggests that DMSO does not dissociate prior to the turnover-limiting step. Application of the steady-state approximation to the Pd^{II}-cyclohexanone adduct results in the rate law shown in eq 8, which is consistent with the first-order dependence on [cyclohexanone] and [Pd(DMSO)$_2$(TFA)$_2$]. Subsequent β-hydride elimination[27] and aerobic oxidation of the Pd^{II}–hydride[16] are rapid and kinetically invisible under the catalytic conditions.

$$\frac{d[\text{cyclohexenone}]}{dt} = \frac{k_1 k_2 [\text{cyclohexanone}][\text{Pd(DMSO)}_2(\text{TFA})_2]}{k_2 + k_{-1}} \quad (8)$$

The comparison of acetate and trifluoroacetate as anionic ligands shows that the Pd(TFA)$_2$-derived catalyst is approximately 3-fold more active. This effect is attributed to the enhanced electrophilicity of the TFA-ligated catalyst, which should favor formation of the cyclohexanone adduct and possibly enhance the rate of C−H cleavage. The maximum rate of cyclohexanone is observed, however, with a 1:1 TFA:OAc ratio. Studies of Pd^{II}-mediated C−H activation have highlighted "concerted metalation–deprotonation" mechanisms in which Pd−C bond formation takes place in concert with C−H deprotonation by a coordinated carboxylate,[28] and we have recently observed a similar beneficial effect of mixed TFA/OAc anionic ligands in Pd-catalyzed C−H activation of arenes.[29] These observations potentially reflect a need to balance the electrophilicity of the Pd^{II} center and the basicity of the carboxylate ligand. On the basis of these considerations and the lack of an inhibitory effect by DMSO, we propose the five-coordinate transition structure **1** for α-C−H cleavage. This

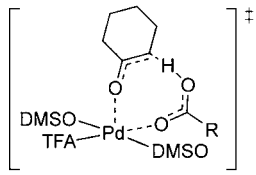

1 R = CH$_3$, CF$_3$

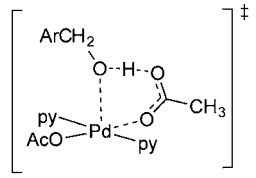

2 py = pyridine

structure closely resembles the five-coordinate transition state **2** proposed for Pd(py)$_2$(OAc)$_2$-catalyzed aerobic oxidation–dehydrogenation of alcohols, which is supported by experimental and DFT computational studies.[30] The initially formed *O*-bound enolate should be able to isomerize readily under the reaction conditions into a *C*-bound enolate that can undergo β-hydride elimination.

A mechanism analogous to Scheme 3, involving a soluble Pd^{II} species, appears to be operative in the dehydrogenation of cyclohexenone during the induction period (cf. Figure 6). The alkene in cyclohexenone is probably a better ligand for Pd than the carbonyl oxygen atom. The resulting alkene adduct may not be on the pathway for α-C−H cleavage, however, and could slow the net dehydrogenation process for this substrate. Furthermore, the loss of DMSO in this step (evident from the inhibitory effect of DMSO) could make the catalyst more susceptible to aggregation into Pd nanoparticles upon reduction to Pd^0. For reasons that have not yet been elucidated, the

dx.doi.org/10.1021/ja4031648 | J. Am. Chem. Soc. 2013, 135, 8205–8212

resulting Pd nanoparticles exhibit higher activity than the molecular Pd^{II} catalyst precursor.

CONCLUSION

$Pd(DMSO)_2(TFA)_2$ catalyzes the chemoselective formation of cyclohexenone, rather than phenol, in the aerobic dehydrogenation of cyclohexanone. The selectivity of this reaction originates from the different kinetic effect of DMSO on the two sequential dehydrogenation steps: DMSO has little impact on the rate of the first dehydrogenation step, whereas it strongly inhibits the second step. DMSO is found to stabilize the homogeneous Pd^{II} catalyst, which mediates efficient ketone-to-enone dehydrogenation. The same catalyst is not effective for cylohexenone-to-phenol dehydrogenation. Efficient catalysis of the latter reaction is only observed under conditions that enable conversion of the homogeneous Pd into Pd nanoparticles. These findings may be compared to our companion study of the $Pd(TFA)_2$/2-Me_2Npy catalyst system, which promotes full dehydrogenation of cyclohexanone to phenol.[17] In this reaction, the Pd^{II} catalyst precursor transforms rapidly into Pd nanoparticles that mediate both dehydrogenation steps. Together, these studies represent a clear demonstration of different selectivity patterns that can arise from homogeneous versus nanoparticle catalysis.[31]

ASSOCIATED CONTENT

Supporting Information

Experimental details for data acquisition and additional kinetic data. This material is available free of charge via the Internet at http://pubs.acs.org.

AUTHOR INFORMATION

Corresponding Author

stahl@chem.wisc.edu

Notes

The authors declare no competing financial interest.

ACKNOWLEDGMENTS

We thank Profs. Hans J. Reich, Clark R. Landis and Tehshik P. Yoon (UW−Madison) for helpful discussions. Financial support of this work was provided by the NIH (R01-GM100143) and NSF (CHE-1041934, to D.P.). The O_2 dependence experiment was performed on a HEL high-pressure ChemSCAN unit, which was funded by the NSF (CHE-0946901).

REFERENCES

(1) For recent reviews: (a) Dobereiner, G. E.; Crabtree, R. H. *Chem. Rev.* **2010**, *110*, 681. (b) Choi, J.; MacArthur, A. H. R.; Brookhart, M.; Goldman, A. S. *Chem. Rev.* **2011**, *111*, 1761.

(2) Recent efforts to use transfer dehydrogenation catalysts with cyclohexanone substrates: (a) Yi, C. S.; Lee, D. W. *Organometallics* **2009**, *28*, 947. (b) Zhang, X.; Wang, D. Y.; Emge, T. J.; Goldman, A. S. *Inorg. Chim. Acta* **2011**, *369*, 253.

(3) For a leading review article, see: (a) Cavani, F.; Ballarini, N.; Cericola, A. *Catal. Today* **2007**, *127*, 113. (b) Gärtner, C. A.; van Veen, A. C.; Lercher, J. A. *ChemCatChem* **2013**, DOI: 10.1002/cctc.201200966.

(4) Muzart, J. *Eur. J. Org. Chem.* **2010**, 3779.

(5) For general reviews of Pd-catalyzed aerobic oxidation reactions, see: (a) Stahl, S. S. *Angew. Chem., Int. Ed.* **2004**, *43*, 3400. (b) Gligorich, K. M.; Sigman, M. S. *Chem. Commun.* **2009**, 3854. (c) Shi, Z.; Zhang, C.; Tang, C.; Jiao, N. *Chem. Soc. Rev.* **2012**, *41*, 3381.

(6) For leading primary references, see: (a) Theissen, R. J. *J. Org. Chem.* **1971**, *36*, 752. (b) Trost, B. M.; Metzner, P. J. *J. Am. Chem. Soc.* **1980**, *102*, 3572. (c) Muzart, J.; Pete, J. P. *J. Mol. Catal.* **1982**, *15*, 373. (d) Wenzel, T. T. *J. Chem. Soc., Chem. Commun.* **1989**, 932. (e) Sheldon, R. A.; Sobczak, J. M. *J. Mol. Catal.* **1991**, *68*, 1. (f) Shvo, Y.; Arisha, A. H. I. *J. Org. Chem.* **1998**, *63*, 5640. (g) Tokunaga, M.; Harada, S.; Iwasawa, T.; Obora, Y.; Tsuji, Y. *Tetrahedron Lett.* **2007**, *48*, 6860. (h) Bercaw, J. E.; Hazari, N.; Labinger, J. A. *J. Org. Chem.* **2008**, *73*, 8654. (i) Williams, T. J.; Caffyn, A. J. M.; Hazari, N.; Oblad, P. F.; Labinger, J. A.; Bercaw, J. E. *J. Am. Chem. Soc.* **2008**, *130*, 2418. (j) Giri, R.; Maugel, N.; Foxman, B. M.; Yu, J.-Q. *Organometallics* **2008**, *27*, 1667. (k) Stang, E. M.; White, M. C. *J. Am. Chem. Soc.* **2011**, *133*, 14892.

(7) Complementary studies have been reported describing hydrogen-atom-abstraction reactions that install sites of unsaturation into organic molecules: (a) Bigi, M. A.; Reed, S. A.; White, M. C. *Nat. Chem.* **2011**, *3*, 216. (b) Voica, A.-F.; Mendoza, A.; Gutekunst, W. R.; Fraga, J. O.; Baran, P. S. *Nat. Chem.* **2012**, *4*, 629.

(8) Izawa, Y.; Pun, D.; Stahl, S. S. *Science* **2011**, *333*, 209.

(9) Diao, T.; Wadzinski, T. J.; Stahl, S. S. *Chem. Sci.* **2012**, *3*, 887.

(10) For a concurrent report on Pd/diazafluorenone-catalyzed dehydrogenation, see: Gao, W.; He, Z.; Qian, Y.; Zhao, J.; Huang, Y. *Chem. Sci.* **2012**, *3*, 883.

(11) Diao, T.; Stahl, S. S. *J. Am. Chem. Soc.* **2011**, *133*, 14566.

(12) (a) Simon, M.-O.; Girard, S. A.; Li, C.-J. *Angew. Chem., Int. Ed.* **2012**, *51*, 7537. (b) Imahori, T.; Tokuda, T.; Taguchi, T.; Takahata, H. *Org. Lett.* **2012**, *14*, 1172. (c) Xie, Y.; Liu, S.; Liu, Y.; Wen, Y.; Deng, G.-J. *Org. Lett.* **2012**, *14*, 1692. (d) Hajra, A.; Wei, Y.; Yoshikai, N. *Org. Lett.* **2012**, *14*, 5488. (e) Girard, S. A.; Hu, X.; Knauber, T.; Zhou, F.; Simon, M.-O.; Deng, G.-J.; Li, C.-J. *Org. Lett.* **2012**, *14*, 5606. (f) Izawa, Y.; Zheng, C.; Stahl, S. S. *Angew. Chem., Int. Ed.* **2013**, *52*, 3672. (g) Sutter, M.; Sotto, N.; Raoul, Y.; Métay, E.; Lemaire, M. *Green Chem.* **2013**, *15*, 347.

(13) Kinetic fitting was carried with COPASI software: Hoops, S.; Sahle, S.; Gauges, R.; Lee, C.; Pahle, J.; Simus, N.; Singhal, M.; Xu, L.; Mendes, P.; Kummer, U. *Bioinformatics* **2006**, *22*, 3067.

(14) The mechanistic insights obtained in the present study suggest that solvents that stabilize homogeneous Pd catalysts will provide better selectivity for enone versus phenol formation. The mechanistic basis for such stabilization effects is not fully known, but multiple factors could contribute. Possible effects include the relative O_2 solubility, the coordinating ability of the solvent, and/or other effects that contribute to the partitioning between catalyst reoxidation by O_2 versus aggregation of Pd^0 into nanoparticles.

(15) (a) Ito, Y.; Hirao, T.; Saegusa, T. *J. Org. Chem.* **1978**, *43*, 1011. (b) Larock, R. C.; Hightower, T. R.; Kraus, G. A.; Hahn, P.; Zheng, D. *Tetrahedron Lett.* **1995**, *36*, 2423. (c) Porth, S.; Bats, J. W.; Trauner, D.; Giester, G.; Mulzer, J. *Angew. Chem., Int. Ed.* **1999**, *38*, 2015.

(16) (a) Popp, B. V.; Stahl, S. S. *J. Am. Chem. Soc.* **2007**, *129*, 4410. (b) Konnick, M. M.; Stahl, S. S. *J. Am. Chem. Soc.* **2008**, *130*, 5753. (c) Popp, B. V.; Stahl, S. S. *Chem.—Eur. J.* **2009**, *15*, 2915. (d) Decharin, N.; Popp, B. V.; Stahl, S. S. *J. Am. Chem. Soc.* **2011**, *133*, 13268. (e) Konnick, M. M.; Decharin, N.; Popp, B. V.; Stahl, S. S. *Chem. Sci.* **2011**, *2*, 326.

(17) Pun, D.; Diao, T.; Stahl, S. S. *J. Am. Chem. Soc.* **2013**, DOI: 10.1021/ja403165u.

(18) The heterogeneous Pd was isolated by filtration through Celite. Efforts to use this material in the dehydrogenation of cyclohexenone under the standard reactions conditions led to disproportionation of cyclohexenone into cyclohexanone and phenol. For a precedent for this disproportionation reactivity with Pd/C, see: Horning, E. C.; Horning, M. G.; Walker, G. N. *J. Am. Chem. Soc.* **1949**, *71*, 169. For similar observations with cyclohexene, see refs 6b and 6i.

(19) Rubottom, G. M.; Gruber, J. M. *J. Org. Chem.* **1977**, *42*, 1051.

(20) Formation of the linear conjugated dienolate can be achieved by using $KN(TMS)_2$ as the base: Kawanisi, M.; Itoh, Y.; Hieda, T.; Kozima, S.; Hitomi, T.; Kobayashi, K. *Chem. Lett.* **1985**, 647.

(21) Forsyth, D. A.; Botkin, J. H.; Osterman, V. M. *J. Am. Chem. Soc.* **1984**, *106*, 7663.

(22) Kasahara, A.; Tanaka, K.; Asamiya, K. *Bull. Chem. Soc. Jpn.* **1967**, *40*, 351.
(23) For related Pd-mediated cleavage of allylic C−H bonds to form π-allyl-Pd complexes, see ref 6b and Parshall, G. W.; Wilkinson, G. *Inorg. Chem.* **1962**, *1*, 896.
(24) The syntheses of 2,6,6-cyclohexenone-d_3 and 2,4,4,6,6-cyclohexenone-d_5 are based on procedures described in following paper: Lambert, J. B.; Clikeman, R. R. *J. Am. Chem. Soc.* **1976**, *98*, 4203. In this paper, 2,6,6-cyclohexenone-d_3 is inaccurately assigned to 2,4,4-cyclohexenone-d_3. Our ^{1}H NMR and 1D NOESY data confirm that the resulting deuterated substrate is 2,6,6-cyclohexenone-d_3.
(25) For reviews, see: (a) Widegren, J. A.; Finke, R. G. *J. Mol. Catal A: Chem.* **2003**, *198*, 317. (b) Crabtree, R. H. *Chem. Rev.* **2011**, *112*, 1536.
(26) Diao, T.; White, P.; Guzei, I.; Stahl, S. S. *Inorg. Chem.* **2012**, *51*, 11898.
(27) For a fundamental study of β-hydride elimination from a Pt^{II}-enolate, see: Alexanian, E. J.; Hartwig, J. F. *J. Am. Chem. Soc.* **2008**, *130*, 15627.
(28) (a) Davies, D. L.; Donald, S. M. A.; Macgregor, S. A. *J. Am. Chem. Soc.* **2005**, *127*, 13754. (b) García-Cuadrado, D.; Braga, A. A. C.; Maseras, F.; Echavarren, A. M. *J. Am. Chem. Soc.* **2006**, *128*, 1066. (c) Gorelsky, S. I.; Lapointe, D.; Fagnou, K. *J. Am. Chem. Soc.* **2008**, *130*, 10848. (d) Balcells, D.; Clot, E.; Eisenstein, O. *Chem. Rev.* **2010**, *110*, 749. (e) Ackermann, L. *Chem. Rev.* **2011**, *111*, 1315.
(29) Izawa, Y.; Stahl, S. S. *Adv. Synth. Catal.* **2010**, *352*, 3223.
(30) Steinhoff, B. A.; Guzei, I. A.; Stahl, S. S. *J. Am. Chem. Soc.* **2004**, *126*, 11268.
(31) Homogeneous vs nanoparticle catalysis was recently invoked to explain a switch in selectivity between alcohol oxidation and Wacker-type oxidation of alkenes: Mifsud, M.; Parkhomenko, K. V.; Arends, I. W. C. E.; Sheldon, R. A. *Tetrahedron* **2010**, *66*, 1040.